

Massive Black Hole formation in proto-stellar clusters via early gas accretion

Zacharias Roupas^{1,2}

¹ Dipartimento di Fisica “G. Occhialini”, Università degli Studi di Milano-Bicocca,
Piazza della Scienza 3, 20126 Milano, Italy

² Istituto Nazionale di Fisica Nucleare (INFN), Sezione di Milano-Bicocca,
Piazza della Scienza 3, 20126 Milano, Italy

Correspondence: zacharias.roupas@unimib.it

Abstract

We review our semi-analytic model of stellar black hole (BH) mass growth by gas accretion in gas-rich stellar clusters during their birthstage within the first ~ 10 Myr after the first stellar formation event. Such proto-stellar clusters are massive and compact, with typical masses $\sim 10^6 M_\odot$ and sizes ~ 1 pc, suggested by recent James Webb Space Telescope (JWST) observations. We find that the BH masses are shifted by the end of gas depletion to values within and above the BH mass gap, well within the range of components of the recent gravitational-wave (GW) signal GW231123, and up to masses $\sim 10^3 M_\odot$.

1 Introduction

In Ref. [1], we proposed a channel for the BH mass growth via gas accretion in proto-stellar clusters to values within the upper BH mass gap, induced by the physics of a pair-instability supernova (PISN) [2–4], $60 M_\odot \lesssim m_{\text{BH}} \lesssim 130 M_\odot$, and up to the intermediate-massive-black-hole (IMBH) regime of $m_{\text{BH}} \sim 10^3 M_\odot$. We review briefly the model and main results here.

Gas-rich, compact, low-metallicity, massive stellar clusters provide ideal conditions for the mass growth of stellar BHs via accretion. Mass segregation, which drives the massive stellar progenitors of BHs toward the dense center of the cluster [5], is accelerated in the presence of ambient gas at timescales $\lesssim 1$ Myr [6]. In addition, a lower-metallicity environment weakens stellar winds, allowing for longer gas-depletion timescales in a sufficiently compact cluster, even if they allow for energetic PISN to occur (which inject significant energy to the ambient gas) [1].

Recent JWST observations revealed five proto-stellar cluster candidates in the Cosmic Gems arc galaxy at high redshift, $z = 10.2$, [7], likely progenitors of globular clusters [8–10]. Their typical masses are $\sim 10^6 M_\odot$ and half-light radii ~ 1 pc, providing observationally motivated cluster parameters for model-building. Our semi-analytic framework of stellar-BH growth in such environments [1] accounts for gas depletion by stellar feedback, gas accretion, distinct BH formation times, dynamical friction, and stochastic kicks induced by stellar encounters and gas turbulence.

Identifying the origin of heavy BHs $\sim 10^2 - 10^3 M_\odot$ is a timely, active area of research [11–28]. The GW experiments, LIGO-Virgo-KAGRA Collaborations, have revealed a significant population of BHs within the upper BH mass gap [29]. The most recent such GW signal, GW231123 [30], involves components which are both heavy, $103_{-52}^{+20} M_\odot$, $137_{-17}^{+22} M_\odot$. Such values are naturally produced in our model. Furthermore, our model offers a pathway toward the formation of IMBH in the early Universe, providing the potential to explain the observed, intriguing, abundance and masses of Supermassive BHs (SMBH) at high redshifts [31–33]. This open issue is also important for the Laser Interferometer Space Antenna (LISA) mission [34].

In the next section we review our cluster and BH motion model. Section 3 presents our results, and we conclude in Section 4.

2 Physical model

2.1 Gas depletion timescale

In a gas-rich cluster, stellar winds and SN explosions inject energy and momentum to the ambient gas, which drive its expulsion out of the cluster. Stellar lifetimes determine both the time when SN occur, and the birth time of BHs from their stellar progenitors. Stellar formation in dense gas is completed rapidly ($\lesssim 1\text{Myr}$) [35, 36], and is therefore justified to assume it occurs in a constant metallicity environment. Note also that stellar winds of solar-type intermediate-mass stars of $m < 8 M_\odot$ contribute negligible energies within the depletion timescales $\sim 10\text{Myr}$ (e.g. [37]), and are therefore neglected. We use phenomenological relations [1] to model stellar winds, SN energy injection, and stellar lifetimes according to observational and numerical data. We estimate the depletion timescale τ as the moment when the accumulated injected energy becomes equal to the initial binding energy of the gas.

We find [1] that the depletion timescale depends primarily on the compactness of the cluster (see also [38])

$$C \equiv \frac{M/10^5 M_\odot}{r_h}, \quad (1)$$

rather than on the cluster mass alone. This is because the binding energy scales as $U \propto C \cdot M$, while the total stellar feedback $E_{\text{feed}} \propto M$ regardless of compactness. In Fig. 1, we display τ as a function of compactness for several values of stellar formation ε , and for low metallicity $Z = 0.01 Z_\odot$. In [1], the reader can find additional figures for solar and sub-solar metallicities. We observe a characteristic stall at

$$\tau_{\text{stall}} \approx 2.9\text{Myr} \quad (2)$$

which marks the onset of PISN. The range of compactness values used in our simulations, and which satisfy the ones of observed proto-stellar clusters in the Cosmic Gems arc galaxy, correspond to this stall timescale.

2.2 Stellar cluster and BH motion

We assume that the background gas and stellar densities follow Plummer profiles. We account for several important physical processes in the cluster: cluster expansion driven by gas mass loss, the greater spatial extent of the gas component relative to the stellar component, the

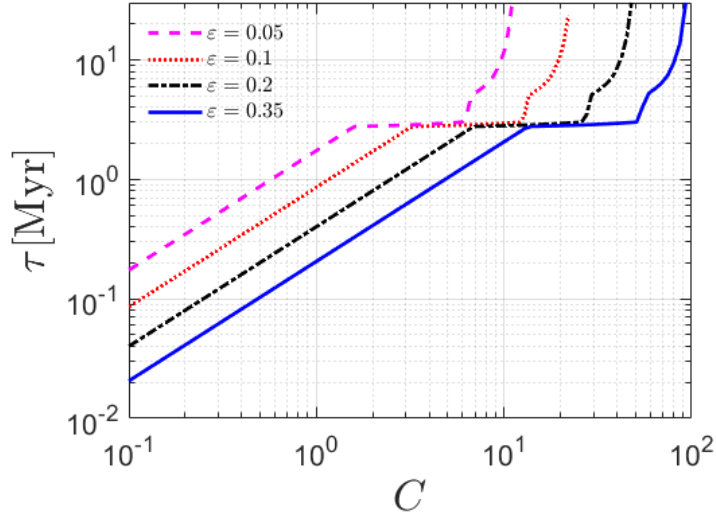


Figure 1: Depletion timescale, τ , with respect to the compactness, C , of a gas-rich stellar cluster of any total mass at low metallicity for different possible star formation efficiencies, ε .

gas temperature profile, and gas cooling over time. We adopt the standard exponential law of gas depletion [39],

$$\frac{dM_{\text{gas}}(t)}{dt} = -\frac{M_{\text{gas}}(t)}{\tau}, \quad (3)$$

since the stellar feedback generates energy proportional to the cluster mass. Each run is terminated once 99% of the initial gas mass has been depleted.

Our adopted initial BH mass function (BHMF) is the Salpeter profile [40]. The BH positions and velocities are sampled from the Brownian probability density of Ref. [41]. Each BH is created at a distinct time based on the zero-age main sequence (ZAMS) progenitor mass. The correspondence of ZAMS progenitor to BH mass is applied according to Figure 2 of Ref. [3]. We classify the BHs on several types depending on the ZAMS progenitors mass: core-collapse-SN (CCSN), direct-collapse of low or high ZAMS mass, and pulsational-pair-instability-SN (PPISN) of low or high ZAMS mass. We impose an upper cut-off on ZAMS mass at $230M_{\odot}$ and a cut-off on the upper initial BH mass at $55M_{\odot}$ as suggested by stellar evolution models [2–4]. This also allows us to isolate the BH gas accretion channel for populating the upper BH mass gap and quantify its sole contribution. Note, however, it has been argued that supermassive stars ($m_{\text{ZAMS}} > 230M_{\odot}$) could be created either by runaway collisions [19, 42–44] or rapid gas accretion [45–47] in stellar clusters. Those stars could potentially generate BHs within the upper BH mass gap via direct collapse. The extent to which such supermassive stars contribute to our proposed BH growth channel warrants further investigation. Nevertheless, since they would only enhance the population of the BH mass gap, our analysis represents a conservative calculation of the BH mass function shift in proto-stellar clusters.

We integrate the BHs equations of motion with a standard drift-kick scheme [1]. The deterministic forces – gravity and dynamical friction from the background – were implemented using a standard Runge-Kutta method. For the dynamical friction induced by the stellar component we use the standard Chandrasekhar formula [48]. The dynamical friction induced by gas requires modification to account for the hydrodynamic nature of the interaction as in Ref [49], while we also include the deceleration due to the mass increase [50–53].

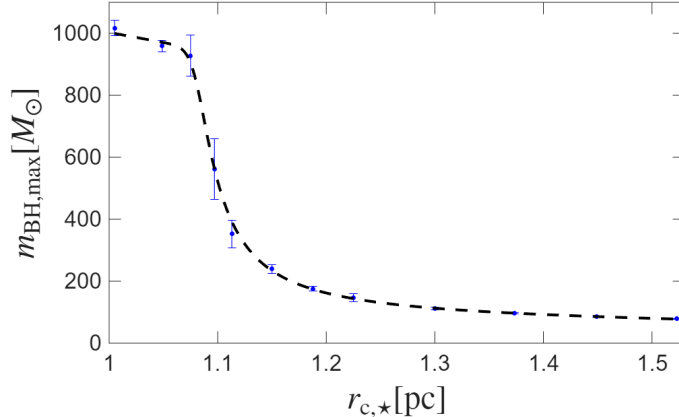


Figure 2: The sample maximum shifted individual BH mass in a stellar cluster with total stellar mass $M_* = 10^6 M_\odot$ and size $r_{c,*} = 1\text{pc}$, values representative of the observed Cosmic Gems proto-stellar clusters. The x -axis is the final, after gas depletion, stellar Plummer radius, to be compared to the half-light radius of the observed stellar clusters.

We applied at adaptive timesteps, stochastic velocity increments, due to both stellar perturbations and gas turbulence. Those timestep values $\Delta t_{\text{stoch}}(r_{\text{BH}}, t)$ are determined dynamically at the end of each previous step by the minimum of the relevant physical timescales, locally for each BH. Those are the dynamical timescale, the crossing timescale, the dynamical friction timescale and the turbulence correlation timescale. We apply bounds $10^{-5} \text{ Myr} \leq \Delta t_{\text{stoch}} \leq 10^{-1} \text{ Myr}$. Those are in effect never violated, since we get in practice that $\Delta t_{\text{stoch}} \approx 10^{-4} - 10^{-2} \text{ Myr}$ for any r_{BH} and t . The stochastic kicks on BHs due to stellar encounters are modelled as a white noise process (e.g. [41]). Gas turbulence on the other hand is modeled as an Ornstein-Uhlenbeck (OU) process acting on the BH through a time-correlated turbulent acceleration field. This OU process is a well-defined stochastic process with a finite autocorrelation timescale and can be used to excite turbulent motions in simulations [54–56]. We integrate the OU stochastic differential equation directly to get the turbulent acceleration and the corresponding velocity kick.

We adopt an isotropic hot-type accretion, whose typical representative is Bondi-Hoyle accretion [57]. The spherically symmetric accretion rate is [58]

$$\dot{m}_{\text{feed}} = \pi \rho_{\text{gas}} v_{\text{rel}} R_{\text{acc}}^2, \quad v_{\text{rel}} = \sqrt{v_\bullet^2 + c_s^2}. \quad (4)$$

The appropriate value of accretion radius, R_{acc} depends on the relative amount of gas and the radial position of the accretor [59]. If the gas dominates the cluster potential at a certain BH position, r_\bullet , the accretion rate is determined by a tidal-lobe accretion radius [60]. Otherwise, when gas is less dominant, the appropriate accretion radius is the Bondi-Hoyle radius [58]. We assume the accretion radius to be the smaller of the two at any instant in time [59] adopting the most conservative assumption. We impose a maximum threshold for accretion rate

$$\dot{m}_{\text{acc}}(t) = \min \{ \dot{m}_{\text{feed}}(t), 10 \dot{m}_{\text{Edd},0} \} \quad (5)$$

where $\dot{m}_{\text{Edd},0} = 4\pi G m_{\text{BH}} m_p / \eta_0 \sigma_T c$ is the reference Eddington rate value for the radiative efficiency $\eta_0 = 0.057$. This is a conservative cap based on the results of [61]. In practice, we find $0 < \dot{m}_{\text{feed}}(t) / \dot{m}_{\text{Edd},0} < 10$, which satisfies the cap automatically.

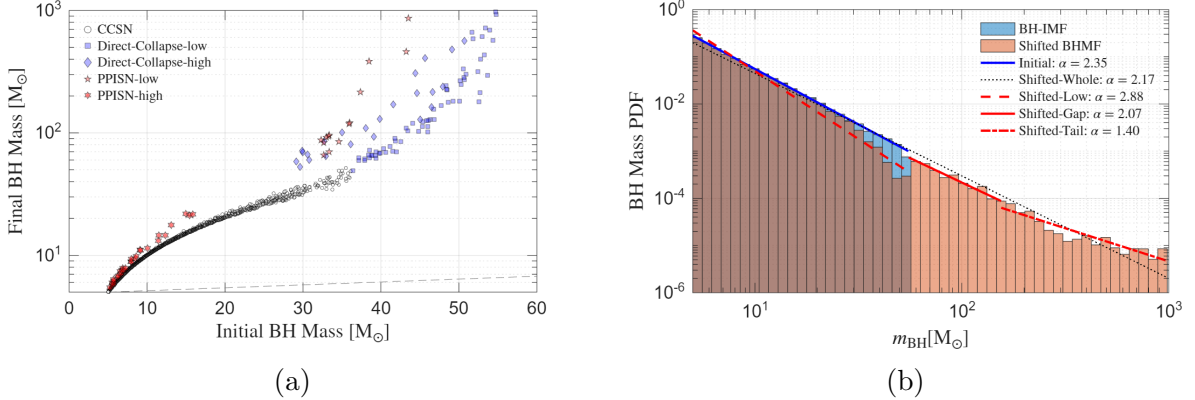


Figure 3: Mass scatter diagram (a), and BH mass function (b), for a cluster with total stellar mass $M_\star = 10^6 M_\odot$ and final size $r_{c,\star} = 1$ pc, representing the observed Cosmic Gems proto-stellar clusters. In (a) the data refers to a single typical simulation. In (b) we use ten samples. The parameter α denotes the exponent of each histogram fit.

3 Results

We model proto-stellar clusters, resembling the observed ones in the Cosmic Gems arc galaxy [7]. Their observed masses range $(1 - 4) \cdot 10^6 M_\odot$ and the half-light radii $(0.7 - 1.7)$ pc. We adopt $\varepsilon = 0.35$ representing the upper end ~ 0.3 of observed star formation efficiencies in embedded clusters [39, 62], appropriate for the extreme densities and low metallicity in such massive, compact proto-stellar clusters. We assume a low metallicity $0.01 Z_\odot$, in accordance with the low metallicity expected for the Cosmic Gems clusters [7].

We choose initial total mass of the gas-rich cluster $M = 3 \cdot 10^6 M_\odot$, which means $M_\star = 10^6 M_\odot$ for the stellar component, that is the low-mass end of the observations. In our investigation, we cover a range of initial half-mass radii $r_h = 0.6 - 1$ pc which result to stellar Plummer radii $r_{c,\star} = 0.9 - 1.6$ pc because of expansion due to mass loss. For all these cluster sizes, the clusters have identical gas depletion timescales $\tau = 2.9$ Myr, which implies that by 13 Myr the 99% of the gas has been expelled when we terminate the simulation.

We find that the upper BH mass gap is populated even for the most conservative cluster sizes. In Figure 2 we depict the maximum individual BH mass with respect to $r_{c,\star}$, to be compared with the observed half-light radius of Cosmic Gems clusters. Remarkably, resulting stellar clusters with $r_{c,\star} \lesssim 1$ pc can host IMBH with mass $\sim 10^3 M_\odot$. In Figure 3 we present the results of ten runs for this typical size. Our empirical general fit of the individual BH mass increase for all BHs, describing the trend of Figure 3a, is

$$\Delta m_{\text{BH}} \approx (m_{\text{BH,birth}}/25M_\odot)^7, \quad (6)$$

where the characteristic mass ranges $\sim (20 - 30) M_\odot$ and the exponent $\sim 6 - 8$ for different cluster sizes. The BHMF shifts to higher masses (Figure 3b) populating the mass-gap with a negative power exponent $\simeq 2.1$ fitted within the mass-gap range. The power exponent of the tail $m_{\text{BH}} > 130 M_\odot$ is 1.4.

4 Discussion and conclusion

We have presented a semi-analytic model of BH mass growth in gas-rich proto-stellar clusters. Our analysis accounts for the gas depletion timescale incorporating stellar lifetimes, stellar

winds, and SN explosions, the generation of realistic BH populations with assigned progenitor masses, the input of BHs into the cluster according to their formation times, and stochastic perturbations from both gas and stellar components. The BH mass growth is found to satisfy a power law $\Delta m = (m_{\text{BH}}(0)/m_c)^\beta$ with parameter values which depend on cluster properties, and take typical values $m_c \sim 25$ and $\beta \sim 7$ for low metallicity clusters with masses $\sim 10^6 M_\odot$ and sizes ~ 1 pc. Our analysis has direct observational implications. The observed Cosmic Gems proto-stellar clusters at high redshift likely experienced early accretion-driven BH mass function shifts to higher masses, generating $\gtrsim 25$ BHs with masses $10^2 M_\odot \lesssim m_{\text{BH}} \lesssim 10^3 M_\odot$ within their first $\lesssim 10$ Myr.

Our mechanism can provide further an explanation for some of the heavy, mass-gap BHs ($> 60 M_\odot$) detected by LIGO-Virgo-KAGRA. The key observable that may allow determine the origin of the BH growth mechanism is BH spin. Particularly, the recent signal GW231123 [30] had masses $m_1 = 137_{-17}^{+22} M_\odot$, $m_2 = 103_{-52}^{+20} M_\odot$, and spins $a_{*,1} = 0.9_{-0.19}^{+0.10}$, $a_{*,2} = 0.8_{-0.51}^{+0.20}$. Let us discuss if our proposed mechanism can provide such high spins. Gas accretion spins up a Schwarzschild BH ($a = 0$) up to an extreme Kerr BH ($a = 1$) after having accreted mass $\sqrt{6} M_\odot$ [63]. A BH that grows within the BH mass gap in our system accretes typically at a rate $2\text{--}10 M_\odot/\text{Myr}$. This implies that it shall reach the maximum spin in a timescale $\lesssim 2$ Myr that is less than the total depletion time-window of ~ 10 Myr. Thus, there is sufficient time for BHs to spin-up at high spin values comparable to GW231123. We are currently working on the modelling of BH spin-up and spin distribution, which will be reported elsewhere [64].

This work opens several avenues for future investigation: (i) the role of our proposed BHMF-shift mechanism in seeding high-redshift SMBH formation, (ii) IMBHs produced through this channel represent promising targets for GW detection by the future LISA mission; (iii) binary BHs which accrete gas generate a GW background, which is important for GW missions, such as LISA; (iv) calculate the, possibly, distinctive spin signature of our mechanism and perform data analysis to distinguish from merger-formed BHs in current and future LIGO-Virgo-KAGRA GW data.

Acknowledgments

This research was supported by the European Union’s Horizon Europe Research and Innovation Programme under the Marie Skłodowska-Curie grant agreement No. 101149270–ProtoBH.

References

- [1] Zacharias Roupas. Black hole mass function shift in proto-stellar clusters driven by gas accretion. *Astron. Astrophys.*, 702:A208, October 2025. doi: 10.1051/0004-6361/202556434.
- [2] K. Belczynski, A. Heger, W. Gladysz, A. J. Ruitter, S. Woosley, G. Wiktorowicz, H. Y. Chen, T. Bulik, R. O’Shaughnessy, D. E. Holz, C. L. Fryer, and E. Berti. The effect of pair-instability mass loss on black-hole mergers. *Astron. Astrophys.*, 594:A97, October 2016. doi: 10.1051/0004-6361/201628980.
- [3] Mario Spera and Michela Mapelli. Very massive stars, pair-instability supernovae and intermediate-mass black holes with the sevn code. *MNRAS*, 470(4):4739–4749, October 2017. doi: 10.1093/mnras/stx1576.

- [4] S. E. Woosley and Alexander Heger. The Pair-instability Mass Gap for Black Holes. *ApJL*, 912(2):L31, May 2021. doi: 10.3847/2041-8213/abf2c4.
- [5] L. Spitzer. *Dynamical evolution of globular clusters*. Princeton University Press, 1987.
- [6] N. W. C. Leigh, A. Mastrobuono-Battisti, H. B. Perets, and T. Böker. Stellar dynamics in gas: the role of gas damping. *MNRAS*, 441:919–932, June 2014. doi: 10.1093/mnras/stu622.
- [7] Angela Adamo et al. Bound star clusters observed in a lensed galaxy 460 Myr after the Big Bang. *Nature*, 632(8025):513–516, August 2024. doi: 10.1038/s41586-024-07703-7.
- [8] J. M. Diederik Kruijssen. Globular clusters as the relics of regular star formation in ‘normal’ high-redshift galaxies. *MNRAS*, 454(2):1658–1686, December 2015. doi: 10.1093/mnras/stv2026.
- [9] Alvio Renzini. Finding forming globular clusters at high redshifts. *MNRAS*, 469(1):L63–L67, July 2017. doi: 10.1093/mnrasl/slx057.
- [10] Bruce G. Elmegreen. Two Thresholds for Globular Cluster Formation and the Common Occurrence of Massive Clusters in the Early Universe. *ApJ*, 869(2):119, December 2018. doi: 10.3847/1538-4357/aaed45.
- [11] Davide Gerosa and Emanuele Berti. Are merging black holes born from stellar collapse or previous mergers? *Phys. Rev. D*, 95(12):124046, June 2017. doi: 10.1103/PhysRevD.95.124046.
- [12] Zacharias Roupas and Demosthenes Kazanas. Generation of massive stellar black holes by rapid gas accretion in primordial dense clusters. *Astron. Astrophys.*, 632:L8, December 2019. doi: 10.1051/0004-6361/201937002.
- [13] Vishal Baibhav, Davide Gerosa, Emanuele Berti, Kaze W. K. Wong, Thomas Helfer, and Matthew Mould. The mass gap, the spin gap, and the origin of merging binary black holes. *Phys. Rev. D*, 102(4):043002, August 2020. doi: 10.1103/PhysRevD.102.043002.
- [14] M. Renzo, M. Cantiello, B. D. Metzger, and Y. F. Jiang. The Stellar Merger Scenario for Black Holes in the Pair-instability Gap. *ApJL*, 904(2):L13, December 2020. doi: 10.3847/2041-8213/abc6a6.
- [15] Chase Kimball, Colm Talbot, Christopher P. L. Berry, Matthew Carney, Michael Zevin, Eric Thrane, and Vicky Kalogera. Black hole genealogy: Identifying hierarchical mergers with gravitational waves. *The Astrophysical Journal*, 900(2):177, sep 2020. doi: 10.3847/1538-4357/aba518. URL <https://dx.doi.org/10.3847/1538-4357/aba518>.
- [16] Mohammadtaher Safarzadeh and Zoltán Haiman. Formation of GW190521 via Gas Accretion onto Population III Stellar Black Hole Remnants Born in High-redshift Minihalos. *ApJL*, 903(1):L21, November 2020. doi: 10.3847/2041-8213/abc253.
- [17] Michela Mapelli, Marco Dall’Amico, Yann Bouffanais, Nicola Giacobbo, Manuel Arca Sedda, M. Celeste Artale, Alessandro Ballone, Ugo N. Di Carlo, Giuliano Iorio, Filippo Santoliquido, and Stefano Tornamenti. Hierarchical black hole mergers in young, globular and nuclear star clusters: the effect of metallicity, spin and cluster properties. *MNRAS*, 505(1):339–358, July 2021. doi: 10.1093/mnras/stab1334.

- [18] Francesco Paolo Rizzuto, Thorsten Naab, Rainer Spurzem, Manuel Arca-Sedda, Mirek Giersz, Jeremiah Paul Ostriker, and Sambaran Banerjee. Black hole mergers in compact star clusters and massive black hole formation beyond the mass gap. *MNRAS*, 512(1): 884–898, May 2022. doi: 10.1093/mnras/stac231.
- [19] Manuel Arca Sedda, Albrecht W. H. Kamlah, Rainer Spurzem, Francesco Paolo Rizzuto, Thorsten Naab, Mirek Giersz, and Peter Berczik. The DRAGON-II simulations - II. Formation mechanisms, mass, and spin of intermediate-mass black holes in star clusters with up to 1 million stars. *MNRAS*, 526(1):429–442, November 2023. doi: 10.1093/mnras/stad2292.
- [20] Stefano Torniamenti, Michela Mapelli, Carole Périgois, Manuel Arca Sedda, Maria Celeste Artale, Marco Dall’Amico, and Maria Paola Vaccaro. Hierarchical binary black hole mergers in globular clusters: Mass function and evolution with redshift. *Astron. Astrophys.*, 688:A148, August 2024. doi: 10.1051/0004-6361/202449272.
- [21] Michiko S. Fujii, Long Wang, Ataru Tanikawa, Yutaka Hirai, and Takayuki R. Saitoh. Simulations predict intermediate-mass black hole formation in globular clusters. *Science*, 384(6703):1488–1492, June 2024. doi: 10.1126/science.adi4211.
- [22] Rujuta A. Purohit, Giacomo Fragione, Frederic A. Rasio, Grayson C. Petter, and Ryan C. Hickox. Binary Black Hole Mergers and Intermediate-mass Black Holes in Dense Star Clusters with Collisional Runaways. *AJ*, 167(5):191, May 2024. doi: 10.3847/1538-3881/ad3103.
- [23] Thomas W. Baumgarte and Stuart L. Shapiro. Boosting the growth of intermediate-mass black holes: Collisions with massive stars. *Phys. Rev. D*, 111(6):063039, March 2025. doi: 10.1103/PhysRevD.111.063039.
- [24] Seungjae Lee, Hyung Mok Lee, Ji-hoon Kim, Rainer Spurzem, Jongsuk Hong, and Eunwoo Chung. Formation and Evolution of Compact Binaries Containing Intermediate-mass Black Holes in Dense Star Clusters. *ApJ*, 988(1):15, July 2025. doi: 10.3847/1538-4357/adde52.
- [25] Imre Bartos and Zoltan Haiman. Accretion is All You Need: Black Hole Spin Alignment in Merger GW231123 Indicates Accretion Pathway. *arXiv e-prints*, art. arXiv:2508.08558, August 2025. doi: 10.48550/arXiv.2508.08558.
- [26] Fulya Kiroğlu, Kyle Kremer, and Frederic A. Rasio. Beyond Hierarchical Mergers: Accretion-driven Origins of Massive, Highly Spinning Black Holes in Dense Star Clusters. *ApJL*, 994(2):L37, December 2025. doi: 10.3847/2041-8213/ae1eeb.
- [27] Ore Gottlieb, Brian D. Metzger, Danat Issa, Sean E. Li, Mathieu Renzo, and Maximiliano Isi. Spinning into the Gap: Direct-horizon Collapse as the Origin of GW231123 from End-to-end General-relativistic Magnetohydrodynamic Simulations. *ApJL*, 993(2): L54, November 2025. doi: 10.3847/2041-8213/ae0d81.
- [28] Shuai Liu, Long Wang, Ataru Tanikawa, Weiwei Wu, and Michiko S. Fujii. On the Formation of GW231123 in Population III Star Clusters. *ApJL*, 993(1):L30, November 2025. doi: 10.3847/2041-8213/ae1024.

- [29] R. Abbott et al. GWTC-3: Compact Binary Coalescences Observed by LIGO and Virgo during the Second Part of the Third Observing Run. *Physical Review X*, 13(4):041039, October 2023. doi: 10.1103/PhysRevX.13.041039.
- [30] A. G. Abac et al. GW231123: A Binary Black Hole Merger with Total Mass 190^{+265}_{-10} M_{\odot} . *ApJL*, 993(1):L25, November 2025. doi: 10.3847/2041-8213/ae0c9c.
- [31] Rebecca L. Larson et al. A CEERS Discovery of an Accreting Supermassive Black Hole 570 Myr after the Big Bang: Identifying a Progenitor of Massive $z \lesssim 6$ Quasars. *ApJL*, 953(2):L29, August 2023. doi: 10.3847/2041-8213/ace619.
- [32] Ákos Bogdán, Andy D. Goulding, Priyamvada Natarajan, Orsolya E. Kovács, Grant R. Tremblay, Urmila Chadayammuri, Marta Volonteri, Ralph P. Kraft, William R. Forman, Christine Jones, Eugene Churazov, and Irina Zhuravleva. Evidence for heavy-seed origin of early supermassive black holes from a $z \approx 10$ X-ray quasar. *Nature Astronomy*, 8(1): 126–133, January 2024. doi: 10.1038/s41550-023-02111-9.
- [33] John Regan and Marta Volonteri. Massive Black Hole Seeds. *The Open Journal of Astrophysics*, 7:72, September 2024. doi: 10.33232/001c.123239.
- [34] Pau Amaro-Seoane et al. Astrophysics with the Laser Interferometer Space Antenna. *Living Reviews in Relativity*, 26(1):2, December 2023. doi: 10.1007/s41114-022-00041-y.
- [35] Lee Hartmann, Javier Ballesteros-Paredes, and Fabian Heitsch. Rapid star formation and global gravitational collapse. *MNRAS*, 420(2):1457–1461, February 2012. doi: 10.1111/j.1365-2966.2011.20131.x.
- [36] Stella S. R. Offner, Josh Taylor, and Michael Y. Grudic. The Life and Times of Star-forming Cores: An Analysis of Dense Gas in the STARFORGE Simulations. *ApJ*, 982(2):138, April 2025. doi: 10.3847/1538-4357/adb71d.
- [37] Claus Leitherer, Daniel Schaerer, Jeffrey D. Goldader, Rosa M. González Delgado, Carmelle Robert, Denis Foo Kune, Duilia F. de Mello, Daniel Devost, and Timothy M. Heckman. Starburst99: Synthesis Models for Galaxies with Active Star Formation. *Astrophys. J. Supp.*, 123(1):3–40, July 1999. doi: 10.1086/313233.
- [38] Martin G. H. Krause, Corinne Charbonnel, Nate Bastian, and Roland Diehl. Gas expulsion in massive star clusters?. Constraints from observations of young and gas-free objects. *Astron. Astrophys.*, 587:A53, March 2016. doi: 10.1051/0004-6361/201526685.
- [39] H. Baumgardt and P. Kroupa. A comprehensive set of simulations studying the influence of gas expulsion on star cluster evolution. *MNRAS*, 380(4):1589–1598, October 2007. doi: 10.1111/j.1365-2966.2007.12209.x.
- [40] Rosalba Perna, Yi-Han Wang, Will M. Farr, Nathan Leigh, and Matteo Cantiello. Constraining the Black Hole Initial Mass Function with LIGO/Virgo Observations. *ApJL*, 878(1):L1, June 2019. doi: 10.3847/2041-8213/ab2336.
- [41] Zacharias Roupas. Gravitational Brownian motion as inhomogeneous diffusion: Black hole populations in globular clusters. *Astron. Astrophys.*, 646:A20, February 2021. doi: 10.1051/0004-6361/202039151.

- [42] Marc Freitag, Frederic A. Rasio, and Holger Baumgardt. Runaway collisions in young star clusters - I. Methods and tests. *MNRAS*, 368(1):121–140, May 2006. doi: 10.1111/j.1365-2966.2006.10095.x.
- [43] Marc Freitag, M. Atakan Gürkan, and Frederic A. Rasio. Runaway collisions in young star clusters - II. Numerical results. *MNRAS*, 368(1):141–161, May 2006. doi: 10.1111/j.1365-2966.2006.10096.x.
- [44] Marcelo C. Vergara et al.
- [45] Takashi Hosokawa, Kazuyuki Omukai, and Harold W. Yorke. Rapidly Accreting Super-giant Protostars: Embryos of Supermassive Black Holes? *ApJ*, 756(1):93, September 2012. doi: 10.1088/0004-637X/756/1/93.
- [46] Y. Sakurai, T. Hosokawa, N. Yoshida, and H. W. Yorke. Formation of primordial supermassive stars by burst accretion. *MNRAS*, 452(1):755–764, September 2015. doi: 10.1093/mnras/stv1346.
- [47] L. Haemmerlé, G. Meynet, L. Mayer, R. S. Klessen, T. E. Woods, and A. Heger. Maximally accreting supermassive stars: a fundamental limit imposed by hydrostatic equilibrium. *Astron. Astrophys.*, 632:L2, December 2019. doi: 10.1051/0004-6361/201936716.
- [48] S. Chandrasekhar. Dynamical Friction. I. General Considerations: the Coefficient of Dynamical Friction. *ApJ*, 97:255, March 1943. doi: 10.1086/144517.
- [49] Eve C. Ostriker. Dynamical Friction in a Gaseous Medium. *ApJ*, 513(1):252–258, Mar 1999. doi: 10.1086/306858.
- [50] T. Tanaka and Z. Haiman. The Assembly of Supermassive Black Holes at High Redshifts. *ApJ*, 696:1798–1822, May 2009. doi: 10.1088/0004-637X/696/2/1798.
- [51] A. T. Lee and S. W. Stahler. Dynamical friction in a gas: the subsonic case. *MNRAS*, 416:3177–3186, October 2011. doi: 10.1111/j.1365-2966.2011.19273.x.
- [52] Aaron T. Lee and Steven W. Stahler. Dynamical friction in a gas: The supersonic case. *Astron. Astrophys.*, 561:A84, Jan 2014. doi: 10.1051/0004-6361/201322829.
- [53] Zacharias Roupas and Demosthenes Kazanas. Binary black hole growth by gas accretion in stellar clusters. *Astron. Astrophys.*, 621:L1, Jan 2019. doi: 10.1051/0004-6361/201834609.
- [54] V. Eswaran and S. B. Pope. An examination of forcing in direct numerical simulations of turbulence. *Computers and Fluids*, 16(3):257–278, January 1988.
- [55] Wolfram Schmidt, Wolfgang Hillebrandt, and Jens C. Niemeyer. Numerical dissipation and the bottleneck effect in simulations of compressible isotropic turbulence. *Computers & Fluids*, 35(4):353–371, 2006. ISSN 0045-7930. doi: <https://doi.org/10.1016/j.compfluid.2005.03.002>. URL <https://www.sciencedirect.com/science/article/pii/S0045793005000563>.
- [56] C. Federrath, J. Roman-Duval, R. S. Klessen, W. Schmidt, and M. M. Mac Low. Comparing the statistics of interstellar turbulence in simulations and observations. Solenoidal versus compressive turbulence forcing. *Astron. Astrophys.*, 512:A81, March 2010. doi: 10.1051/0004-6361/200912437.

- [57] David Merritt. *Dynamics and Evolution of Galactic Nuclei (Princeton Series in Astrophysics)*. Princeton University Press, 2013. ISBN 069112101X.
- [58] Juhan Frank, Andrew King, and Derek J. Raine. *Accretion Power in Astrophysics: Third Edition*. Cambridge University Press, 2002.
- [59] I. A. Bonnell, C. J. Clarke, M. R. Bate, and J. E. Pringle. Accretion in stellar clusters and the initial mass function. *MNRAS*, 324(3):573–579, Jun 2001. doi: 10.1046/j.1365-8711.2001.04311.x.
- [60] B. Paczyński. Evolutionary Processes in Close Binary Systems. *Ann. Rev. Astron. Astrophys.*, 9:183, Jan 1971. doi: 10.1146/annurev.aa.09.090171.001151.
- [61] Kohei Inayoshi, Zoltán Haiman, and Jeremiah P. Ostriker. Hyper-Eddington accretion flows on to massive black holes. *MNRAS*, 459(4):3738–3755, July 2016. doi: 10.1093/mnras/stw836.
- [62] Charles J. Lada and Elizabeth A. Lada. Embedded Clusters in Molecular Clouds. *Ann. Rev. Astron. Astrophys.*, 41:57–115, January 2003. doi: 10.1146/annurev.astro.41.011802.094844.
- [63] James M. Bardeen. Kerr Metric Black Holes. *Nature*, 226(5240):64–65, April 1970. doi: 10.1038/226064a0.
- [64] Z. Roupas. Spin-up and spin distribution of stellar black holes grown by gas accretion in proto-stellar clusters. *to appear*, 2026.